Universal Journal of Environmental Research and Technology
 eISSN 2249 0256
Available Online at: www.environmentaljournal.org
Volume 1, Issue 4: 515-530

Open Access **Research Article**

Calcareous Soil as a New Adsorbent to Remove Lead from Aqueous Solution: Equilibrium, Kinetic and Thermodynamic Study

[1]Das B. and [2*]Mondal N. K.

[1] Research Scholar, Department of Environmental Science, The University of Burdwan, India.
[2]Department of Environmental Science, The University of Burdwan, India.

***Corresponding author: nabakumar_mondal@indiatimes.com**

Abstract:

In this work the feasibility of employing calcareous soil to remove lead (II) ions from its aqueous solutions was investigated under batch mode. The influence of solution pH, sorbent dose, initial lead (II) concentration, contact time, stirring rate and temperature on the removal process were investigated. The lead adsorption was favored with maximum adsorption at pH 6.0. Sorption equilibrium time was observed in 60 min. The equilibrium adsorption data were analyzed by the Freundlich, Langmuir, Dubinin-Radushkevich (D-R) and Temkin adsorption isotherm models. The kinetics of Pb(II) ion was discussed by pseudo-first-order, pseudo-second-order, intra-particle diffusion and surface mass transfer models. It was shown that the adsorption of lead ions could be described by the pseudo-second order kinetic model. The activation energy of the adsorption process (E_a) was found to be -34.64 kJ mol^{-1} by using the Arrhenius equation, indicating exothermic nature of lead adsorption onto calcareous soil. Thermodynamic quantities such as Gibbs free energy ($\triangle G^o$), the enthalpy ($\triangle H^o$) and the entropy change of sorption ($\triangle S^o$) have also been evaluated and it has been found that the adsorption process was spontaneous, feasible and exothermic in nature. A six layered feed forward neural network with back propagation training algorithm was developed using thirty one experimental data sets obtained from laboratory batch study. The ANN predicted results were compared with the experimental results of the laboratory test. It was concluded that calcareous soil has potential for application as an effective adsorbent for removal of lead ions from aqueous solution.

Keywords: Adsorption, Calcareous soil, Isotherms, Kinetics, Thermodynamics, Neural network.

1. Introduction:

Nowadays pollution due to heavy metal contaminants from aqueous solutions is one of the most important environmental concerns due to their high toxicity and impact on human health. Lead (II) is known to be one of the heavy metals and is widely used in many industries including painting, petrochemical, newsprint, smelting, metal electroplating, mining, plumbing and battery industries. The effluents from these industries usually contain considerable amount of lead, which ultimately spreads into the environment through soils and water streams and finally accumulates along the food chain which causes human health hazards. The higher concentration of lead will cause severe damage to the nervous system and affects the function of brain cells (Ho *et al*., 2001). It is also a general metabolic poison and enzyme inhibitor (Li *et al*., 2002). The permissible level for lead in drinking water is 0.05 mg/L. The permissible limit (mg/L) for Pb(II) in wastewater according to Bureau of Indian Standards (BIS) is 0.1 mg/L.(BIS, 1981). Therefore, the concentrations of these metals must be reduced to levels that satisfy environmental regulations for various bodies of water. The conventional methods for removing heavy metal ions from water and wastewater include chemical precipitation, ion-exchange, electrochemical deposition, solvent extraction, membrane filtration and adsorption. Among these, adsorption is effective and economical (Ahmad *et al*., 2009). Many heavy metal adsorption studies have focused on the application of activated carbons (Kikuchi *et al*., 2006; Malik *et al*., 2002). However, it is quite expensive with ralatively high operating costs. Hence there is a growing demand to find low cost and efficient adsorbents to remove heavy metals from aqueous solution. A number of researchers have utilised wide variety of adsorbents to remove heavy metal ions from aqueous solutions. Some of the recent developments include adsorbents like sawdust (Rafatullah *et al*., 2009), rice husk (Akhtar *et al*, 2010), cocoa pod husk (Odoemelam *et al.,* 2011), Clay (Papini *et al*., 2002),

Slag (Dimitrova and Mehandgiev, 1998), peat (Blais *et al*., 2002), goethite (Abdel-Samad and Watson, 1998), gibbsite (Weerasooriya *et al*., 2001)), red mud (Gupta *et al*., 2001), lateritic minerals (Ahmad *et al*., 2002), activated phosphate (Moufilh *et al*., 2005) etc. for the removal of lead ions from aqueous solution.

In this study, calcareous soil which was obtained from Birbhum district, West Bengal, India will be investigated as a potential and low cost adsorbent for the removal of Pb (II) ions from aqueous solutions. The objective of the present work was to study the possibility of utilizing calcareous soil as a sorbent for removing lead ions from aqueous solutions. The effect of various experimental parameters such as adsorbent dose, initial lead (II) concentration, contact time, stirring rate, temperature and pH has been investigated. Adsorption kinetics, isotherms and thermodynamic parameters were also evaluated and reported.

2. Materials and Methods:

2.1 Preparation of the Synthetic Sample:

All the reagents used for the current investigation were of GR grade from E. Merck Ltd., India. A lead nitrate ($Pb(NO_3)_2$) stock solution of 100 mg/L concentration was prepared and the working solutions were made by diluting the former with double distilled water. The range in concentrations of lead (II) ions prepared from standard solution varied between 25 to 100 mg/L. Before mixing the adsorbent, the pH of each lead solution was adjusted to the required value by 0.1 M NaOH or 0.1 M HCl solution.

2.2 Adsorbent collection and preparation:

Calcareous soil used in this study was collected from Birbhum district, West Bengal, India. The soil sample was not purified prior to usage. It was initially sun-dried for 7 days followed by drying in hot air oven at 383 ± 1K for 2 days. The dried soil was crushed and sieved to give a fraction of 150 mesh screen and then stored in sterile, closed glass bottles and used as an adsorbent.

2.3 Analysis:

Adsorbent characterization was performed by means of spectroscopic and quantitative analysis. The pH of aqueous slurry was determined by soaking 1g of soil in 50 ml distilled water, stirred for 24 h and filtered and the final pH was measured. The physico-chemical characteristics of the adsorbent were determined using standard procedures (Saha and Sanyal, 2010). The cation exchange capacity (CEC) of the calcareous soil sample was determined by the ammonium acetate method (Rhoades, 1982). The concentrations of sodium and potassium were estimated by Flame Photometer (Model No. SYSTRONICS 126) while magnesium, calcium and residual lead (II) concentration were determined by atomic absorption spectrophotometer (Model No. GBC HG 3000). For stirring purpose magnetic stirrer (TARSONS, Spinot digital model MC02, CAT No. 6040, S. No. 173) is used. The pH of zero-point charge or pH_{ZPC} was determined based on the previous method (Mondal, 2009). The Fourier transform infrared (FTIR) spectra of calcareous soil was recorded with Fourier transform infrared spectrophotometer (PERKIN-ELMER, FTIR, Model-RX1 Spectrometer, USA) in the range of 400-4,000 cm^{-1}. X-ray diffraction analysis of the adsorbent was carried out using X-ray diffractometer equipment (Model Philips PW 1710) with a Cobalt target at 40 kV. In addition, scanning electron microscopy (SEM) analysis was carried out using a scanning electron microscope (HITACHI, S-530, Scanning Electron Microscope and ELKO Engineering, B.U. BURDWAN) at 20 kV to study the surface morphology of the adsorbent.

2.4 Batch Sorption Experiment:

The batch tests were carried out in glass-stoppered, Erlenmeyer flasks with 50 mL of working volume, with a concentration of 25 mg/L. A weighed amount (2.0g) of adsorbent was added to the solution. The flasks were agitated at a constant speed of 800 rpm for 90 minute in a magnetic stirrer at 313 K. The influence of pH (2.0–8.0), initial lead concentration (25, 50, 75, 100 mg/L), contact time (5, 10, 15, 20, 25, 30, 45, 60, 90 min), adsorbent dose (0.5, 1, 2, 2.5 g/50 ml), and temperature (308, 313, 318, 323, 328, 333 K) were evaluated during the present study. Samples were collected from the flasks at predetermined time intervals for analyzing the residual lead concentration in the solution. The residual amount of lead in each flask was investigated using atomic absorption spectrophotometer. The amount of lead ions adsorbed in milligram per gram was determined by using the following mass balance equation:

$$q_e = \frac{(C_i - C_e)V}{m} \quad (1)$$

where q_e is the amount of lead ion adsorbed onto per unit weight of the adsorbent in mg/g, C_i is the initial concentration of metal ion in mg/L, C_e is the equilibrium metal ion concentration in mg/L, V is the volume of adsorbate in liter and m is the weight of the adsorbent in grams. The percentage of removal of lead ions was calculated from the following equation:

$$\text{Removal (\%)} = \frac{(C_i - C_e)}{C_i} \times 100 \quad (2)$$

3. Results and Discussion:

3.1 Characterization of calcareous soil:

The calcareous soil was found to be stable in water, dilute acids and bases. The adsorbent behaves as neutral at pH zero charge. To understand the adsorption mechanism, it is necessary to determine the point of zero charge (pHzpc) of the adsorbent. Adsorption of cation is favored at pH > pHzpc, while the adsorption of anion is favored at pH< pHzpc (Mondal, 2009). The point of zero charge is 5.5 (figure 1). The physico-chemical properties of calcareous soil are summarized in Table 1.

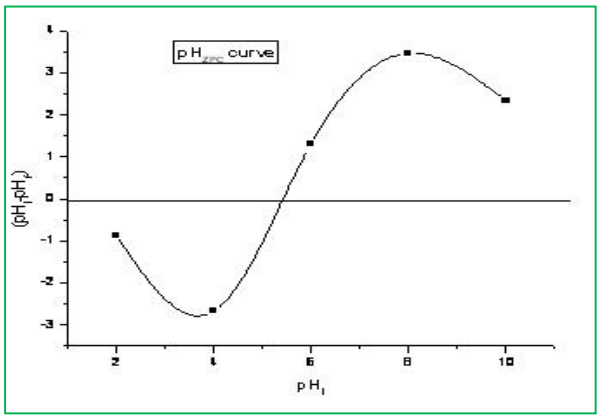

Figure 1: pH of zero point charge of calcareous soil (experimental conditions: adsorbent dose: 1.5 g in 100 ml, Temperature: 313K)

The FTIR spectrum of calcareous soil (figure 2) displays a number of absorption peaks indicating the presence of different types of functional groups. The broad and strong band at 3443 cm^{-1} indicates the presence of –OH groups on the adsorbent surface while peaks at 2927 and 2852 cm^{-1} are related to the C-H vibration of CH_3 and CH_2 groups of side chains and aromatic methoxyl groups. The strong peak at 1637 cm^{-1} shows the presence of carbonate group. The characteristic band at 1105 cm^{-1} corresponds to C-O stretching vibration. The peak at 1032 cm^{-1} indicate the presence of P=O group. The two strong peaks at 698 and 539 cm^{-1} show the presence of C-Cl stretching and C-Br stretching vibration. Hence FTIR spectral analysis demonstrates the existence of negatively charged groups like CH_2, $–CO_3$, -OH, -Cl, -Br on the surface of calcareous soil.

Table 1: Characteristics of calcareous soil

Analysis	Value
pH_{zpc}	5.5
Specific gravity	0.846
Particle size (μm)	150
Moisture content (%)	1.17
Bulk density (g cm^{-3})	0.802
Particle density (g cm^{-3})	1.075
Porosity (%)	25.4
Conductivity (mS/m)	2.0
Cation exchange capacity (meq g^{-1})	36
Na^+ (mg L^{-1})	12.2
K^+ (mg L^{-1})	49.95
Ca^{2+} (meq/100 g)	6.0
Mg^{2+} (meq/100 g)	4.0

3.2 Effect of Initial Lead (II) Ion Concentration:

The rate of adsorption is a function of the initial concentration of the adsorbate, which makes it an important factor to be considered for effective adsorption. The effect of different initial lead (II) ion concentration on adsorption of lead (II) ion onto calcareous soil is presented in figure 6. The percentage removal of lead (II) ion decreased with the increment of the initial lead (II) ions concentration. This can be explained that all adsorbents have a limited number of active sites and at a certain concentration the active sites become saturated (Tsai and Chen, 2010). However, the adsorption capacity at equilibrium increased with increase in initial lead (II) ion concentration. This is due to increasing concentration gradient which acts as increasing driving force to overcome the resistances to mass transfer of lead ion between the aqueous phase and the solid phase (Baek *et al*., 2010). Similar results were obtained in the adsorption of copper and lead ions by manganese oxide coated sand (Han *et al*., 2006).

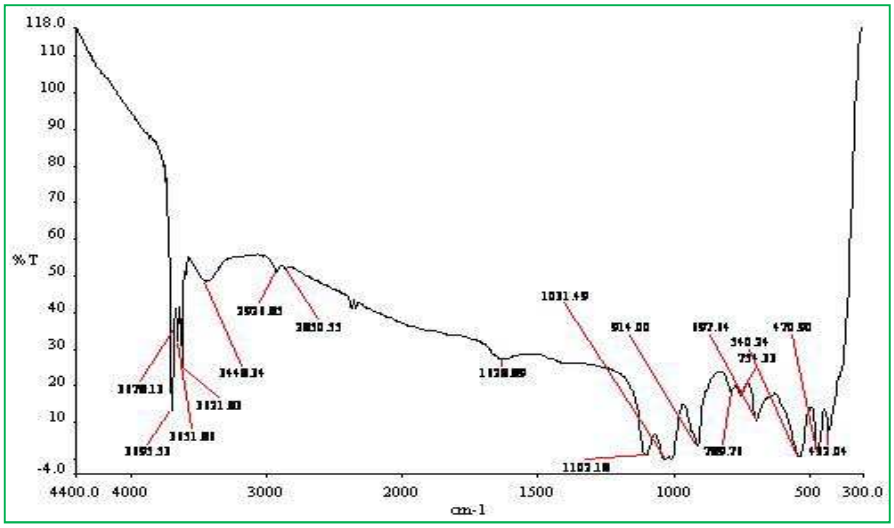

Figure 2: FTIR spectrum of calcareous soil

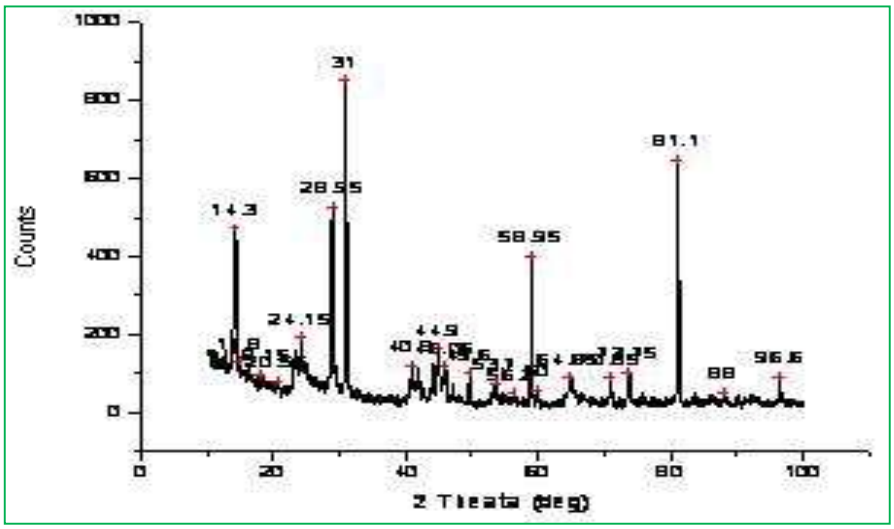

Figure 3: XRD pattern of the adsorbent

X-ray diffraction spectrum of the adsorbent is given in figure 3. The intense main peak shows the presence of highly organized crystalline structure of calcareous soil (Renmin *et al.,* 2005). SEM analysis is another useful tool for the analysis of the surface morphology of an adsorbent. The SEM images for calcareous soil surface before and after lead adsorption are shown in figures 4 and 5 respectively. The porous and irregular surface structure of the adsorbent can be clearly observed in the SEM images shown in figure 4. As can be observed from figure 4 and figure 5 there is clear demarcation in the surface morphology of calcareous soil after treatment.

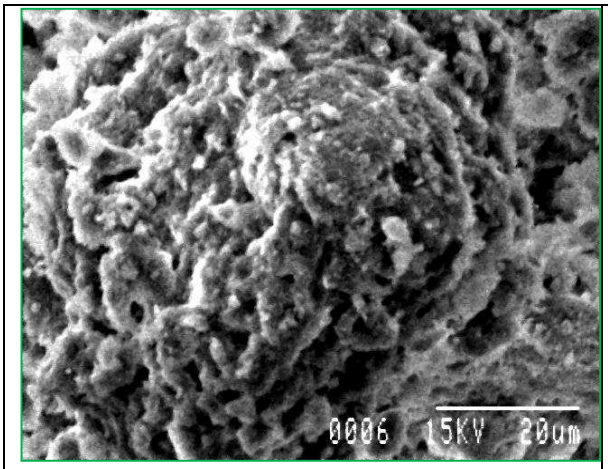

Figure 4: SEM image of calcareous soil before adsorption

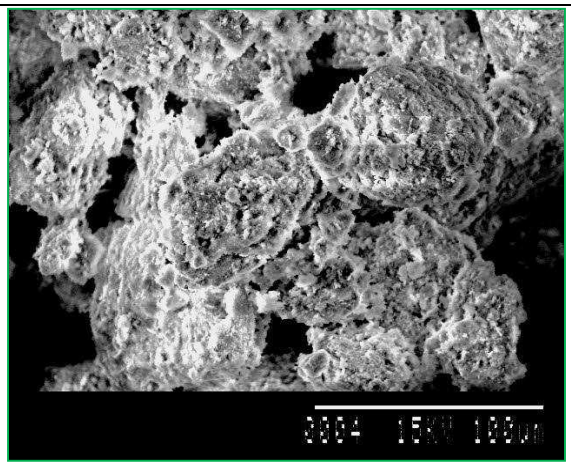

Figure 5: SEM image of calcareous soil after adsorption

3.3 Effect of pH:

The pH of the solution is one of the most critical parameters in the adsorption process, which affects surface charge of the adsorbent material and the degree of ionization and specification of adsorbate (Imamoglu and Tekir., 2008). The effect of pH on the removal efficiency of lead (II) ion was studied at different pH ranging from 2.0 to 8.0. Results are shown in figure 7. It was observed that a sharp increase in the lead ion removal occurred when the pH value of the solutions changed from 2.0 to 6.0. The maximum adsorption of lead ions are obtained at pH 6.0. So pH 6.0 was selected as optimum pH for lead ion adsorption onto calcareous soil. From pH 6 onwards a steady decrease of adsorption of lead ions were recorded. Again the FTIR spectral analysis indicates the presence of –OH and carbonate functional groups onto adsorbent surface (figure 2). This –OH and carbonate groups are protonated at lower pH and thereby restrict the approach of positively charged metal ions to the surface of the adsorbent which results in lower uptake of metal. With decrease in acidity of the solution, the functional group on the adsorbent surface become de-protonated resulting in an increase in the negetive charge density on the adsorbent surface and facilitate the binding of metal cations. The increase in lead (II) ion removal efficiency at higher pH may also be attributed to the reduction of H^+ ions which compete with metal cations at lower pH (Ofomaja *et al*., 2010). Similar observation has been reported for sorption of lead onto Mansonia wood sawdust (Ofomaja *et al*., 2010).

3.4 Effect of Adsorbent Dose:

In this study, five different adsorbent dosages were selected ranging from 0.5 to 2.5 g while the lead concentration was fixed at 25 mg/L. The results are presented in figure 8. It was observed that percentage of lead ion removal increased with increase in adsorbent dose. Such a trend is mostly attributed to an increase in the sorptive surface area and the availability of more active binding sites on the surface of the adsorbent (Nasuha *et al*., 2010). However, the equilibrium adsorption capacity showed an opposite trend. As the adsorbent dosage was increased from 0.5 to 2.5 g, the adsorption capacity reduced to 2.215 and 0.499 mg g^{-1}, respectively. This may be due to the decrease in total adsorption surface area available to lead ion resulting from overlapping or aggregation of adsorption sites (Crini *et al*., 2007; Akar *et al*., 2009). Thus with increasing the adsorbent mass the amount of lead ion adsorbed onto unit mass of adsorbent gets reduced, thus causing a decrease in q_e value with increasing adsorbent mass concentration. Furthermore maximum lead ion removal (99.99%) was recorded by 2.0 g calcareous soil and further increase in adsorbent dose did not significantly change the adsorption yield. This is due to the non-availability of active sites on the adsorbent and establishment of equilibrium between the lead ion on the adsorbent and in the solution.

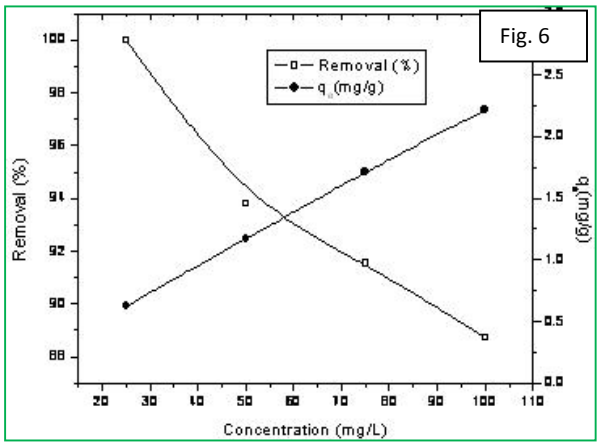

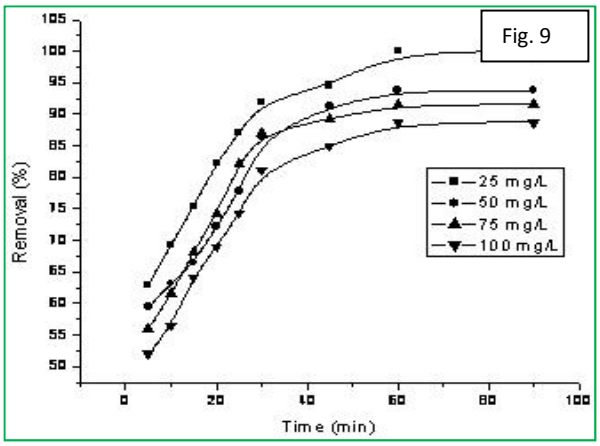

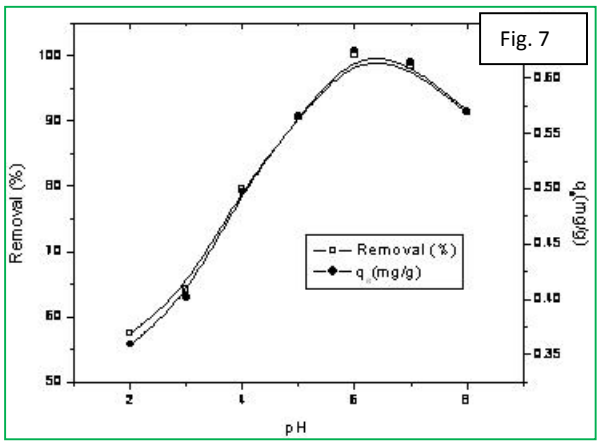

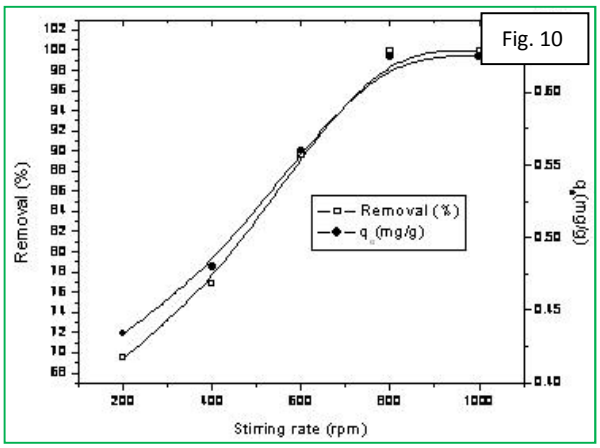

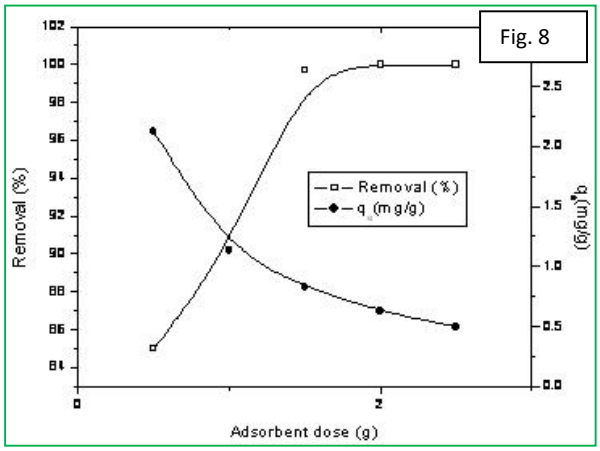

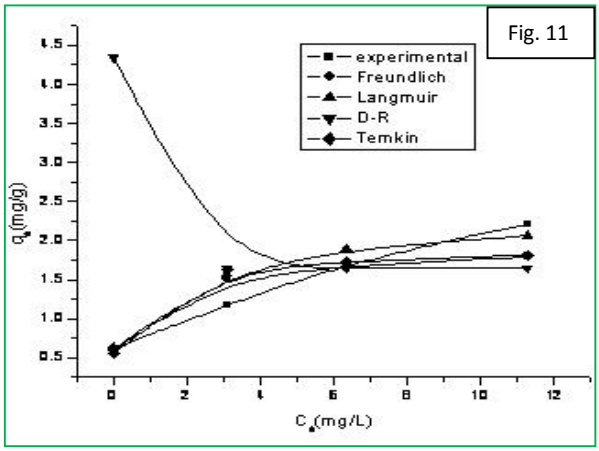

Figure 6: Effect of initial concentration on lead adsorption (experimental conditions: adsorbent dose: 2 g/ 50 ml, agitation speed: 800 rpm, pH: 6.0, Temperature: 313K, Contact time: 60 min)

Figure 7: Effect of pH on lead adsorption (experimental conditions: Initial lead concentration: 25 mg/L, adsorbent dose: 2g/50 ml, agitation speed: 800 rpm, Temperature: 313K, Contact time: 60 min)

Figure 8: Effect of adsorbent dose on lead adsorption (experimental conditions: Initial lead concentration: 25 mg/L, agitation speed: 800 rpm, pH:6.0, Temperature: 313K, Contact time: 60 min)

Figure 9: Effect of contact time on lead adsorption (experimental conditions: Initial lead concentration: 25 mg/L, adsorbent dose: 2g/50 ml, agitation speed: 800 rpm, pH:6.0, Temperature: 313K)

Figure 10: Effect of stirring rate on lead adsorption (experimental conditions: Initial lead concentration: 25 mg/L, adsorbent dose: 2g/50 ml, pH: 6.0, Contact time: 60 min, Temperature: 313K)

Figure 11: Comparison between the measured and modelled isotherm profiles for the adsorption of lead ions by calcareous soil (experimental conditions: adsorbent dose:2.0 g/50 ml, agitation speed: 800 rpm, pH: 6.0, contact time: 60 min, temperature: 313 K)

3.5 Effect of Contact Time:

The uptake of lead (II) ion as a function of contact time is shown in figure 9. The removal rate was rapid initially and then gradually diminished to attain an equilibrium time beyond which there was no significant increase in the rate of removal. The equilibrium was nearly reached after 60 min for four different initial lead (II) ion concentrations. Hence, in the present work, 60 min was chosen as the equilibrium time. The fast adsorption rate at the initial stage may be explained by an increased availability in the number of active binding sites on the adsorbent surface. The sorption rapidly occurs and normally controlled by the diffusion process from the bulk to the surface. In the later stage the sorption is likely an attachment-controlled process due to less available sorption sites. Similar findings for lead (II) adsorption onto other adsorbents have been reported by other investigators (Onundi *et al.,* 2011; Kannan and Veemaraj, 2009; Badmus *et al.,* 2007).

3.6 Effect of Stirring Rate:

The effect of stirring rate on lead adsorption is shown in figure 10 and it appears that stirring rate has pronounced effect on the amount of lead adsorbed. As the stirring rate increased from 200 to 1000 rpm, the adsorption capacity increased from 0.434 to 0.625 mg g^{-1}. However beyond 800 rpm, the adsorption capacity remained constant and the stirring rate of 800 rpm was selected in subsequent analysis. The increase in adsorption capacity at a higher stirring rate could be explained in terms of the reduction of boundary layer thickness around the adsorbent particles (Hanafiah *et al*., 2009). Therefore near the adsorbent surface the concentrations of lead ions would be increased. A higher stirring rate also encourages a better mass transfer of lead ions from bulk solution to the surface of the adsorbent and shortened the adsorption equilibrium time.

3.7 Adsorption Isotherms:

An adsorption isotherm represents the equilibrium relationship between the adsorbate concentration in the liquid phase and that on the adsorbents surface at a given condition. A number of isotherms have been developed to describe equilibrium relationships. In the present study, Langmuir, Freundlich, Temkin, Dubinin-Radushkevich (D-R) models were used to describe the equilibrium data. The results are shown in Table 2 and the modeled isotherms are plotted in figure 11.

3.7.1 The Langmuir Isotherm Model

The Langmuir isotherm model (Langmuir, 1918) was used to describe observed sorption phenomena and suggests that uptake occurs on a homogeneous surface by monolayer sorption without interaction between adsorbed molecules. The linear form of the equation can be written as:

$$\frac{1}{q_{eq}} = \frac{1}{q_{max} K_L C_e} + \frac{1}{q_{max}} \quad (3)$$

where C_e is the equilibrium concentration of Pb(II) (mg/L), q_{eq} is the amount of metal adsorbed per specific amount of adsorbent (mg/g), q_{max} is the maximum adsorption capacity (mg/g), and k_L is an equilibrium constant (L/mg) related to energy of adsorption which quantitatively reflects the affinity between the adsorbent and adsorbate. Where q_{max} and k_L can be determined from the linear plot of $1/q_{eq}$ vs $1/C_e$. The shape of the Langmuir isotherm can be used to predict whether a sorption system is favorable or unfavorable in a batch adsorption process. The essential features of the isotherm can be expressed in terms of a dimensionless constant separation factor (R_L) that can be defined by the following relationship (Anirudhan and Radhakrishnan, 2008).

$$R_L = \frac{1}{1 + K_L C_i} \quad (4)$$

where C_i is the initial concentration (mg/L) and k_L is the Langmuir equilibrium constant (L/mg). The value of separation parameter R_L provides important information about the nature of adsorption. The value of R_L indicated the type of Langmuir isotherm to be irreversible (R_L=0), favourable (0<R_L<1), linear (R_L=1) or unfavourable (R_L>1). It can be explained apparently that when k_L > 0, sorption system is favorable (Chen *et al*., 2008).The evaluated constants are given in Table 2.

3.7.2 The Freundlich Isotherm Model:

The Freundlich isotherm is applicable to non-ideal adsorption on heterogeneous surfaces and the linear form of the isotherm can be represented as (Freundlich, 1906):

$$\mathbf{logq_{eq} = logK_F + \frac{1}{n} logC_e} \quad (5)$$

where, K_F is the Frumdlich constant related to sorption capacity (mg/g) $(L/g)^{1/n}$ and n is related to the adsorption intensity of the adsorbent. Where, K_F and 1/n can be determined from the linear plot of log q_{eq} versus log C_e . The evaluated constants are given in Table 2.

3.7.3 The Temkin Isotherm Model:

Temkin isotherm model was also used to fit the experimental data. Unlike the Langmuir and Freundlich equation, the Temkin isotherm takes into account the interactions between adsorbents and metal ions to be adsorbed and is based on the assumption that the free energy of sorption is a function of the surface coverage (Chen *et al*., 2008). The linear form of the Temkin isotherm is represented as:

$$\mathbf{q_e = BlnA + BlnC_e} \quad (6)$$

where C_e is concentration of the adsorbate at equilibrium (mg/L), q_e is the amount of adsorbate adsorbed at equilibrium (mg/g), $RT/b_T = B$ where T is the temperature (K), and R is the ideal gas constant (8.314 J mol^{-1} K^{-1}) and A and b_T are constants. A plot of q_e versus lnC_e enables the determination of constants A and B. The constant B is related to the heat of adsorption and A is the equilibrium binding constant (L/min) corresponding to the maximum binding energy. The values of A and B are given in Table 2.

3.7.4 The Dubinin-Radushkevich Isotherm Model:

The Dubinin-Radushkevich model (Dubinin *et al*., 1947) was chosen to estimate the heterogeneity of the surface energies. The linear form of D-R isotherm equation is represented as:

$$\mathbf{lnq = lnq_m - \beta\epsilon^2} \quad (7)$$

$$\mathbf{\epsilon = RT\ ln\ (1 + \frac{1}{C_e})} \quad (8)$$

where q_m is the theoretical saturation capacity (mol/g), β is a constant related to the mean free energy of adsorption per mole of the adsorbate (mol^2/J^2), and ε is the polanyi potential, C_e is the equilibrium concentration of adsorbate in solution (mol/L), R (J mol^{-1} K^{-1}) is the gas constant and T(K) is the absolute temperature. The D-R constants q_m and β were calculated from the linear plots of lnq_e versus ε^2 and are given in Table 2. The constant β gives an idea about the mean free energy E (kJ/mol) of adsorption per molecule of the adsorbate when it is transferred to the surface of the solid from infinity in the solution and can be calculated from the relationship (Kundu and Gupta, 2006)

$$\mathbf{E = \frac{1}{\sqrt{2\beta}}} \quad (9)$$

If the magnitude of E is between 8 and 16 kJ mol^{-1}, the sorption process is supposed to proceed via chemisorption, while for values of E 〈 8 kJ mol^{-1}, the sorption process is of physical nature (Kundu and Gupta, 2006).

3.8 Error analysis:

Due to the inherent bias resulting from linearization, four different error functions of non-linear regression basin [sum of the square of the errors (SSE), sum of the absolute errors (SAE) and chi-square (χ^2)] were employed in this study to find out the best-fit isotherm model to the experimental equilibrium data.

SSE is given as:

$$\mathbf{SSE} = \sum_{i=1}^{n} (q_{e,estm} - q_{e,\exp})_i^2 \quad (10)$$

Here, $q_{e,estm}$ and $q_{e,exp}$ are, respectively, the estimated and the experimental value of the equilibrium adsorbate solid concentration in the solid phase (mg/g), and n is the number of the data point.

SAE is given as:

$$\mathbf{SAE} = \sum_{i=1}^{n} \left| q_{e,estm} - q_{e,\exp} \right|_i \quad (11)$$

Chi-square (χ^2) is given as:

$$\boldsymbol{\chi^2} = \sum_{i=1}^{n} \left[\frac{(q_{e,\exp} - q_{e,estm})^2}{q_{e,estm}} \right]_i \quad (12)$$

The respective values are given in the Table 2.

Table 2: Adsorption isotherm constants for adsorption of lead (II) onto calcareous soil

Langmuir isotherm parameters						
q_{max}(mg/g)	**K_L (L/mg)**		**R^2**	**χ^2**	**SSE**	**SAE**
2.34	0.666		0.918	0.131	0.217	0.735
Freundlich isotherm parameters						
K_F (mg/g)(L mg^{-1})$^{1/n}$	**n**		**R^2**	**χ^2**	**SSE**	**SAE**
1.315	7.69		0.873	0.178	0.298	0.833
Temkin parameters						
B (mg/g)	**A**		**R^2**	**χ^2**	**SSE**	**SAE**
0.150	16.317x10^3		0.739	0.221	0.371	0.936
D-R isotherm parameters						
q_m (mg/g)	**β (mol^2kJ^{-2})**	**E(kJ/mol)**	**R^2**	**χ^2**	**SSE**	**SAE**
1.647	0.004	11.18	0.774	3.527	14.434	4.843

As shown in Table 2, it was observed that the Langmuir isotherm showed good fit to the experimental equilibrium adsorption data than the Freundlich, Dubinin-Radishkevich and Tempkin isotherm equation for Pb (II) sorption according to the values of R^2, χ^2, SSE and SAE. It was also seen from Table 2 that the Langmuir maximum adsorption capacity q_{max} (mg/g) is 2.34 and the equilibrium constant K_L (L/ mg) is 0.666. The separation factor (R_L) values are 0.056, 0.029, 0.019 and 0.014 while initial Pb(II) concentrations are 25, 50, 75 and 100 mg/L, respectively. All the R_L values were found to be less than one and greater than zero indicating the favorable sorption of Pb(II) onto calcareous soil surface. The Freundlich constant K_F indicates the sorption capacity of the sorbent and the value of K_F is 1.315 mg/g. Furthermore, the value of 'n' at equilibrium is 7.69. The value of n lies between 1 and 10 indicating favorable adsorption (Slejko, 1985). From D-R isotherm the value of the adsorption energy was found to be 11.18 kJ/mol. The estimated value of E for the present study was found in the range expected for chemical adsorption (Table 2). Thus the sorption of Pb(II) on the surface of calcareous soil was chemical in nature. The effectiveness of calcareous soil as an adsorbent for lead adsorption was also compared with other reported adsorbents. The maximum adsorption capacity obtained in this study is comparable with other adsorbents as shown in Table 3.

3.9 Adsorption Kinetics Modelling:

In order to analyze the rate of adsorption and possible adsorption mechanism of lead onto ASBR, The Lagergren first order (Lagergren, 1898), pseudo-second-order (Ho and Mckay, 2000) Intraparticle diffusion (Weber and Morris, 1963) and surface mass transfer models (Mckay *et al*., 1981) were applied to adsorption data.

3.9.1 The Pseudo-First-Order Kinetic Model:

The Lagergren first order rate equation is represented as:

$$\log (q_e - q_t) = \log q_e - \frac{k_1 t}{2.303} \qquad (13)$$

where q_e and q_t are the amounts of lead adsorbed (mg/g) at equilibrium and at time t, respectively and k_1 is the Lagergren rate constant of first order adsorption (min^{-1}). Values of q_e and k_1 at different concentrations were calculated from the slope and intercept of the plots of log (q_e –q_t) versus t (figure 12). The respective values are given in the Table 4 .

3.9.2 The Pseudo-Second-Order Kinetic Model:

The pseudo-second- order kinetic model which is based on the assumption that chemisorption is the rate-determining step can be expressed as:

$$\frac{t}{q_t} = \frac{1}{k_2 q_e^2} + \frac{t}{q_e} \qquad (14)$$

where k_2 is the rate constant of second order adsorption (g/mg/min). Values of k_2 and q_e were calculated from the plots of t/q_t versus t (figure 13). The respective constant values are given in Table 4 . Furthermore the plot of t/q_t versus t at different temperatures is shown in figure 14 and the pseudo-second-order model constants at different temperatures were presented in the Table 5. The initial adsorption rate, h (mg g^{-1} min^{-1}) at different temperatures was calculated using Eq. (15) (Sari *et al*., 2010) from the pseudo-second-order kinetic parameters and are presented in Table 5.

$$h = k_2 q_e^2 \qquad (15)$$

Table 3: A comparisons of maximum adsorption capacities for lead ions by different adsorbents

Adsorbents	q_{max} (mg/g)	References
Activated carbon	6.68	Mishra and Patel, 2009
Kaolin	4.50	Mishra and Patel, 2009
Saraca indica leaf powder	1.19	Goyal *et al*., 2008
Rolling mill scale	2.74	Martin *et al*., 2005
Bagasse flyash	2.50	Gupta and Ali, 2004
Periwinkle shell carbon	0.0558	Badmus *et al*., 2007
Tea waste	2.0	Ahluwalia and Goyal, 2005
Manganese oxide coated zeolite	1.117	Han *et al*., 2006.
Calcareous soil	2.34	This study

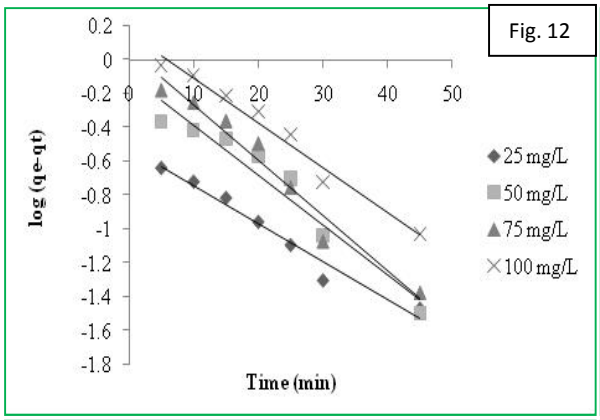

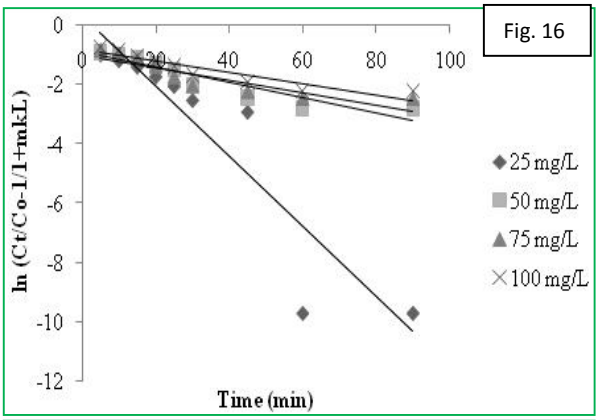

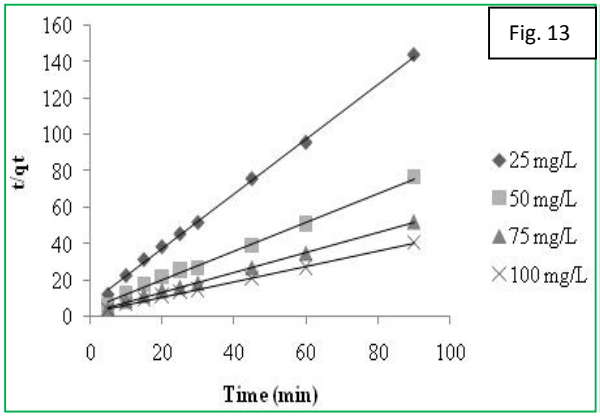

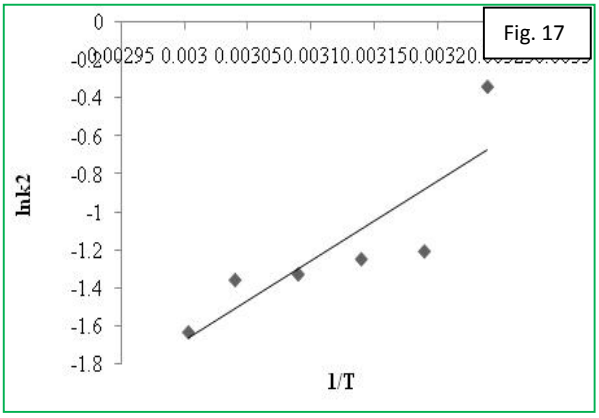

Figure 12: Pseudo first-order kinetic plots for adsorption of lead onto calcareous soil (experimental conditions: adsorbent dose: 2 g/ 50 ml, agitation speed: 800 rpm, pH:6.0, Temperature: 313K)

Figure 13: Pseudo second- order kinetic plots for adsorption of lead onto calcareous soil (experimental conditions: adsorbent dose: 2 g/ 50 ml, agitation speed: 800 rpm, pH:6.0, Temperature: 313K)

Figure 14: Pseudo second- order kinetic plots for adsorption of lead onto calcareous soil at different temperatures (experimental conditions: Initial concentration: 25 mg/L, adsorbent dose: 2 g/ 50 ml, agitation speed: 800 rpm, pH: 6.0)

Figure 15: Intraparticle diffusion model for adsorption of lead onto calcareous soil (experimental conditions: adsorbent dose: 2 g/ 50 ml, agitation speed: 800 rpm, pH:6.0, Temperature: 313K)

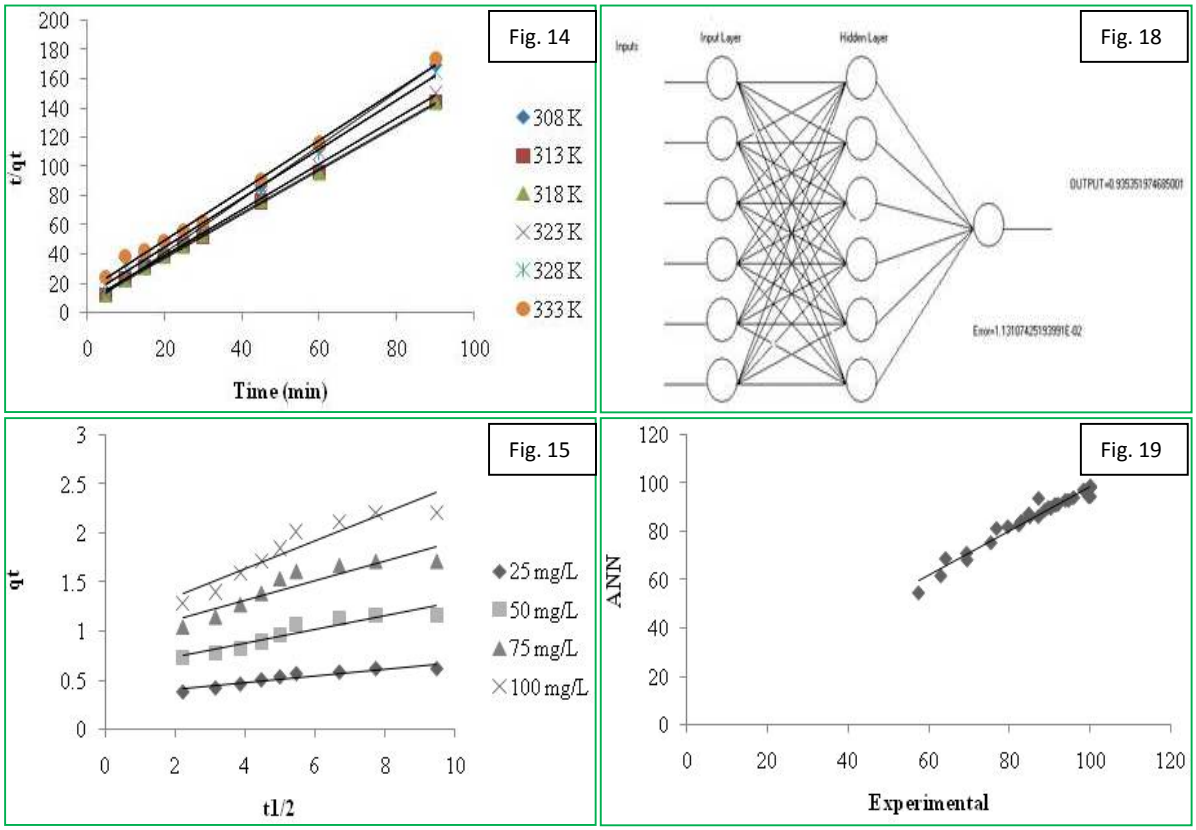

Figure 16: Mass transfer plot for the adsorption of lead on calcareous soil (experimental conditions: initial lead ion concentration: 25 mg L^{-1},adsorbent dose: 2 g/ 50 ml, agitation speed: 800 rpm, pH: 6.0, Temperature: 313 K)

Figure 17: Arrhenius equation plot for adsorption of lead onto calcareous soil

Figure 18: Neural Network architecture

Figure 19: Comparison of experimental data and the simulation results in the training step (R^2=0.959)

3.9.3 The Intraparticle Diffusion Model:

The kinetic results were analyzed by the Weber and Morris intraparticle diffusion model to elucidate the diffusion mechanism. The model is expressed as:

$$q_t = K_d\ t^{1/2} + I \qquad (16)$$

where I is the intercept and K_d is the intra-particle diffusion rate constant. The intercept of the plot reflects the boundary layer effect. Larger the intercept, greater is the contribution of the surface sorption in the rate controlling step. Figure 15 presents intra-particle plot for lead(II) onto calcareous soil. The calculated diffusion coefficient K_d values are listed in Table 4. The K_d value was higher at the higher concentrations. Intraparticle diffusion is the sole rate-limiting step if the regression of q_t versus $t^{1/2}$ is linear and passes through the origin. Infact, the linear plots at each concentration did not pass through the origin. This deviation from the origin is due to the difference in the rate of mass transfer in the initial and final stages of the sorption. This indicated the existence of some boundary layer effect and further showed that intraparticle diffusion was not the only rate-limiting step.

3.9.4 Surface Mass Transfer Kinetic Model:

Mass transfer analysis for the removal of lead was carried out using the kinetic model which describes the transfer of adsorbate in solution. The model is expressed as:

$$\ln\left(\frac{C_t}{C_0} - \frac{1}{1+mk_L}\right) = \ln\frac{mk_L}{1+mk_L} - \frac{1+mk_L}{mk_L}\beta_L S_S\, t \qquad (17)$$

where C_t is the concentration after time t (mg/L), C_o is the is the initial concentration (mg/L), m is the mass of adsorbent per unit volume of particle-free adsorbate solution (g/L), β_L is the mass transfer coefficient (cm/s), k_L is the constant obtained from the Langmuir isotherm equation (L/g), and S_s is the outer surface of adsorbent per unit volume of particle free solution (cm^{-1}), given as:

$$S_S = \frac{6m}{D_a d\,(1-\varepsilon)} \quad (18)$$

where D_a is the particle mean diameter (cm), d is the density of the adsorbent (g/cm^3) and ε is the porosity of the adsorbent. The results are showing in figure 16. The plot of $\ln\left(\frac{C_t}{C_0} - \frac{1}{1+mk_L}\right)$ versus t gives a straight line and thus confirms the validity of the equation for the present system. The value of β_L for different initial concentrations was determined from the slope and intercept of the plots and are shown in Table 4.

Table 4: Kinetic parameters for adsorption of lead (II) onto calcareous soil

Kinetic model	parameters	Concentration of lead (II) solution			
		25 mg/L	50 mg/L	75 mg/L	100 mg/L
	$q_{e,exp}$ (mg/g)	0.625	1.172	1.7165	2.2185
Pseudo-first-order	k_1(min^{-1})	0.050	0.066	0.073	0.06
	$q_{e,cal}$ (mg/g)	0.306	0.812	1.150	1.438
	R^2	0.967	0.939	0.962	0.973
Pseudo-second-order	k_2 (g/mg^{-1} min^{-1})	0.299	0.135	0.109	0.066
	$q_{e,cal}$ (mg/g)	0.663	1.262	1.831	2.398
	R^2	0.998	0.996	0.998	0.997
Intraparticle diffusion	K_d (mg/g.min$^{1/2}$)	0.034	0.069	0.1	0.14
	I	0.347	0.607	0.923	1.08
	R^2	0.882	0.883	0.836	0.882
Surface mass transfer	β_L (cm/s)	8.6x10^{-6}	0.514x10^{-6}	0.391x10^{-6}	0.36x10^{-6}
	R^2	0.851	0.862	0.793	0.849

Table 5: Pseudo-second-order kinetic parameters at different temperatures

T(K)	$q_{e,cal}$ (mg g^{-1})	k_2 (g mg^{-1} min^{-1})	h (mg g^{-1} min^{-1})
308	0.547	0.712	0.213
313	0.663	0.299	0.131
318	0.6605	0.287	0.125
323	0.638	0.265	0.107
328	0.593	0.257	0.090
333	0.581	0.195	0.065

It is clear from the Table 4 that the pseudo- second-order kinetic model showed excellent linearity with high correlation coefficient (R^2>0.99) at all the studied concentrations in comparison to the other kinetic models. In addition the calculated q_e values also agree with the experimental data in the case of pseudo-second-order kinetic model. Therefore it could be concluded that the rate-limiting step of Pb(II) adsorption onto calcareous soil may be chemisorption. It is also evident from Table 4 that the values of the rate constant k_2 decrease with increasing initial Pb(II) concentrations. This is due to the lower competition for the surface active sites at lower concentration but at higher concentration the competition for the surface active sites will be high and consequently lower sorption rates are obtained. Again as shown in Table 4 the external mass transfer coefficient ranges from 8.6x10^{-6} cm/s for 25 mg/L initial Pb(II) and 0.36x10^{-6} cm s^{-1} for 100 mg/L Pb(II) concentration. It was found that the increasing of the initial concentration results in a decreasing of the external mass transfer coefficient. These results are consistent with previous studies on copper and mercury sorption onto chitosan (Mckay *et al*., 1986). It is also observed from Table 5 that rate constant, k_2 decreased as the temperature increased indicating exothermic nature of adsorption of lead ion onto calcareous soil surface. Again as evident from Table 5, the initial adsorption rate, h, decreased with increase in temperature suggesting that adsorption of lead ion onto calcareous soil was not favorable at higher temperatures.

3.10 Activation Energy and Thermodynamic Parameters:

In order to study the feasibility of the adsorption process, the thermodynamic parameters such as free energy, enthalpy and entropy changes can be estimated from the following equations (Sujana *et al*., 2009):

$$K_C = \frac{C_{Ae}}{C_e} \quad (19)$$

$$\Delta G^0 = -RT\ln K_C \quad (20)$$

$$\mathbf{logK_C} = \frac{\Delta \mathbf{S^0}}{\mathbf{2.303R}} - \frac{\Delta \mathbf{H^0}}{\mathbf{2.303RT}} \quad (21)$$

where C_e is the equilibrium concentration in solution in mg/L and C_{Ae} is the equilibrium concentration on the sorbent in mg/L and K_c is the equilibrium constant. The Gibbs free energy (ΔG^o) for the adsorption of lead onto calcareous soil at all temperatures was obtained from Eq. 20 and are presented in Table 6. The values of ΔH^o and ΔS^o were calculated from the slope and intercept of the plot $\log K_c$ against 1/T (figure not shown) and are also listed in Table 6.

From the pseudo-second-order rate constant k_2 (Table 5), the activation energy E_a for the adsorption of lead ions on calcareous soil surface was determined using the Arrhenius equation

$$\mathbf{lnk} = \mathbf{lnA} - \frac{\mathbf{E_a}}{\mathbf{RT}} \quad (22)$$

where k is the rate constant, A is the Arrhenius constant, E_a is the activation energy (kJ mol^{-1}), R is the gas constant (8.314 J mol^{-1} K^{-1}) and T is the temperature (K). By plotting $\ln k_2$ versus 1/T, E_a was obtained from the slope of the linear plot (figure 17) and is presented in Table 6.

Table 6: Thermodynamic parameters for adsorption of lead (II) onto calcareous soil

Temperature (K)	ΔG^o (kj/mol)	ΔH^o (kj/mol)	ΔS^o (kj/mol)	E_a (kj/mol)
		-121.89	-0.347	-34.64
308	-4.39			
313	-23.966			
318	-14.807			
323	-8.441			
328	-5.231			
333	-4.377			

From Table 6 it is clear that the reaction is spontaneous in nature as $\triangle G^o$ values are negative at all the temperature studied. Increase in value of $\triangle G^o$ with increase in temperature suggests that lower temperature makes the adsorption easier. Again negative $\triangle H^o$ value confirms that the sorption is exothermic in nature. The type of sorption can be explained in terms of the magnitude of $\triangle H^o$. The heat evolved during physisorption generally lies in the range of 2.1-20.9 kj mol^{-1}, while the heats of chemisorption falls into a range of 80-200 kj mol^{-1} (Liu and Liu, 2008). Therefore lead sorption onto calcareous soil surface may be attributed to a chemical adsorption process. The negative value of $\triangle S^o$ suggests that the adsorption process is enthalpy driven. The E_a value calculated from the slope of the plot (figure 17) was found to be -34.64 kj/mol. The negative value of E_a indicates that lower solution temperatures favours metal ion removal by adsorption onto the calcareous soil surface and the adsorption process is exothermic in nature.

3.11 Artificial Neural Network modelling (ANN):

A neural network is a massively parallel distributed processor made up of simple processing units, which has a natural propensity for storing experimental knowledge and making it available for use. Neural Network Toolbox Neuro Solution 5 ® mathematical software was used to determine Pb (II) adsorption efficiency. Figure 18 shows the ANN model used in this study. The input vectors, 31 set of experimental data contain pH, initial concentration of Pb (II), adsorbent dosage, time, stirring rate and temperature. There is just one neuron in output layer which is the amount of adsorption. The standardized back-propagation algorithm was used for the training of the input data. The Figure 19 shows the plot of amount of adsorption predicted by ANN versus amount of adsorption obtained from experiments, during the training process. The slope of the line=0.915 and amount R^2 = 0.959 show good training of the network.

4. Conclusion:

In this study, natural calcareous soil of Indian origin was tested and evaluated as a possible adsorbent for removal of lead from its aqueous solution using batch sorption technique. The adsorption process is also dependent on numerous factors such as the solution pH, adsorbent dosage, temperature, stirring rate, initial Pb (II) concentration and contact time. The percentage removal of lead ions decreased with an increase in the lead concentration while it increased with increase in contact time and adsorbent dose upto a certain level. The maximum removal was found at pH 6.0. Equilibrium data fitted very well in the Langmuir isotherm equation,

confirming the monolayer adsorption capacity of Pb(II) ions onto calcareous soil with a monolayer adsorption capacity of 2.34 mg/g at 313 K. According to Dubinin-Radushkevich (D-R) isotherm model, adsorption of lead onto calcareous soil was chemisorption. The adsorption kinetics followed pseudo-second-order kinetic model with a good correlation. Intra-particle diffusion was not the sole rate controlling factor. The activation energy of the adsorption process (E_a) was found to be -34.64 kJ mol^{-1} by using the Arrhenius equation, indicating exotherrmic nature of lead adsorption onto calcareous soil. Thermodynamic analysis suggests that the removal of lead from aqueous solution by calcareous soil was a spontaneous and exothermic process. A comparison between the ANN model simulated results and the experimental data gave high correlation coefficient (R^2 = 0.959). Therefore the present findings suggest that calcareous soil may be used as an inexpensive and effective adsorbent without any treatment or any other modification for the removal of lead ions from aqueous solutions.

Acknowledgements:

The authors are grateful to Dr. Aloke Ghosh, Reader, Department of Chemistry, Burdwan University, West Bengal, India for recording FTIR data and they also extend their gratitude to Dr. Srikanta Chakraborty, Incharge of SEM, USIC, University of Burdwan, West Bengal for SEM study.

References:

1) Abdel-Samad, H. and Watson, P. R. (1998): An XPS study of the adsorption of lead on goethite (α-FeOOH). *Appl. Surf. Sci.,* 136 (1-2): 46–54 .
2) Ahluwalia, S. S. and Goyal, D. (2005): Removal of heavy metals by waste tea leaves from aqueous solution. *Eng. Life Sci.,* 5 (2): 158–162.
3) Ahmad, A. *et al.* (2009): Removal of Cu(II) and Pb(II) ions from aqueous solutions by adsorption onto sawdust of meranti wood. *Desalination,* 247 (1-3): 636–646.
4) Ahmad, S., Khalid, N. and Daud, M. (2002): Adsorption studies of lead on lateritic minerals from aqueous media. *Sep. Sci. Technol.,* 37 (2): 343-362.
5) Akar, S. T. *et al.* (2009): Biosorption of a reactive textile dye from aqueous solutions utilizing an agro-waste. *Desalination,* 249 (2): 757–761.
6) Akhtar, M. *et al.* (2010): An economically viable method for the removal of selected divalent metal ions from aqueous solutions using activated rice husk. *Colloids Surf. B: Biointerf.,* 75 (1): 149–155.
7) Anirudhan, T. S. and Radhakrishnan, P. G. (2008): Thermodynamics and kinetics of adsorption of Cu (II) from aqueous solutions onto a new cation exchanger derived from tamarind fruit shell. *J. Chem. Thermodynamics,* 40 (4): 702-709.
8) Badmus, M. A. O., Audu, T. O. K. and Anyata, B. U. (2007): Removal of lead ion from industrial wastewaters by activated carbon prepared from periwinkle Shells (*Typanotonusfuscatus*). *Turkish J. Eng. Env. Sci.,* 31 (4): 251 – 263
9) Baek, M. H. *et al.* (2010): Removal of Malachite Green from aqueous solution using degreased coffee bean. *J. Hazard. Mater.,* 176 (1-3): 820–828.
10) BIS. (1981): Tolerance limits for industrial effluents prescribed by Bureau of Indian Standards, IS 2490 (Part I), New Delhi.
11) Blais, J. F., Mercier, G. and Durand, A. (2002): Lead and zinc recovery by adsorption on peat moss during municipal incinerator used lime decontamination. *Environ. Technol.,* 23 (5): 515–524.
12) Chen, Z., Ma, W. and Han, M. (2008): Biosorption of nickel and copper onto treated alga(*Undariapinnarlifida*): Application of isotherm and kinetic models. *J. Hazard. Mater.,* 155 (1-2): 327-333.
13) Crini, G. *et al.* (2007): Removal of C.I. Basic Green 4 (Malachite Green) from aqueous solutions by adsorption using cyclodextrin-based adsorbent: kinetic and equilibrium studies. *Sep. Purif. Technol.,* 53 (1): 97–110.
14) Dimitrova, S. V. and Mehandgiev, D. R. (1998): Lead removal from aqueous soluitons by granulated blast- furnace slag. *Wat. Res.,* 32 (11): 3289–3292.
15) Dubinin, M. M., Zaverina, E. D. and Radushkevich, L. V. (1947): Sorption and structure of active carbons. Adsorption of organic vapors. *J. Phy. Chem.,* 21: 1351-1362.
16) Freundlich, H. M. F. (1906): Over the adsorption in solution. *J. Phys. Chem.,* 57: 385- 471.
17) Goyal, P. *et al.* (2008): Saraca indica leaf powder for decontamination of lead: removal, recovery, adsorbent characterization and

equilibrium modeling. *Int. J. Environ. Sci. Technol.,* 5 (1): 27–34.

18) Gupta, V. K. and Ali, I. (2004): Removal of lead and chromium from wastewater using bagasse fly ash-a sugar industry waste. *J. Colloid Interface Sci.,* 271 (2): 321–328.
19) Gupta, V. K., Gupta, M. and Sharma, S. (2001): Process development for the removal of lead and chromium from aqueous solutions using red mud – an aluminium industry waste. *Wat. Res.,* 35(5): 1125–1134.
20) Han, R. *et al.* (2006): Removal of copper (II) and lead (II) from aqueous solution by manganese oxide coated sand: II. Equilibrium study and competitive adsorption. *J. Hazard. Mater*., 137 (1): 480-488.
21) Han, R. *et al.* (2006): Copper (II) and lead (II) removal from aqueous solution in fixed-bed columns by manganese oxide coated zeolite. *J. Hazard.Mat.,* 137 (2): 934-942.
22) Hanafiah, M. A. K., Zakaria, H. and Wan Ngah, W. S. (2009): Preparation, Characterization, andadsorption behavior of Cu (II) ions on to alkali-treated weed (*Imperata cylindrica*) leaf powder. *Water Air Soil Pollut.,* 201 (1-4): 43-53.
23) Ho, Y. S. and Mckay, G. (2000): The kinetics of sorption of divalent metal ions onto sphagnum moss peat. *Wat. Res.,* 34 (3), 735-742.
24) Ho, Y.S., Ng, J.C.Y. and McKay, G. (2001): Removal of lead (II) from effluents by sorption on peat using second-order kinetics. *Separ. Sci. Technol.,* 36 (2): 241–261.
25) Imamoglu, M. and Tekir, O. (2008): Removal of copper (II) and lead (II) ions from aqueous solutions by adsorption on activated carbon from a new precursor hazelnut husks. *Desalination,* 228 (1-3): 108–113.
26) Kannan, N. and Veemaraj, T. (2009): Removal of Lead (II) Ions by adsorption onto bamboo dust and commercial activated carbons -A Comparative Study**.** *E-J. Chem.,* 6(2): 247-256.
27) Kikuchi, Y. *et al.* (2006): Effect of ZnO loading to activated carbon on Pb (II) adsorption from aqueous solution. *Carbon,* 44 (2): 195–202.
28) Kundu, S. and Gupta, A. K. (2006): Arsenic adsorption onto iron oxide-coated cement (IOCC): regression analysis of equilibrium data with several isotherm models and their optimization. *Chem. Eng. J.,* 122 (1-2): 93-106.
29) Lagergren, S. (1898): About the theory of so-called adsorption of soluble substances, der Sogenanntenadsorption geloster stoffe Kungliga Svenska Vetenska psalka de Miens Handlingar. 24: 1-39.
30) Langmuir, I. (1918): The adsorption of gases on plane surfaces of glass, mica and platinum. *J. Am. Chem. Soc.,* 40: 1361-1368.
31) Li, Y.H. *et al.* (2002): Lead adsorption on carbon nanotubes. *Chem. Phys. Lett.,* 357 (3-4): 263–266.
32) Liu, Y. and Liu, Y. J. (2008): Biosorption isotherms, kinetics and thermodynamics. *Sep. Purif. Technol.,* 61 (3): 229–242.
33) Malik, D.J. *et al.* (2002): Characterisation of novel modified active carbons and marine algal biomass for the selective adsorption of lead. *Wat. Res.,* 36 (6): 1527–1538.
34) Martin, M. I. *et al.* (2005): Adsorption of heavy metals from aqueous solutions with by-products of the steelmaking industry. *J. Chem. Technol. Biotechnol.,* 80 (11): 1223–1229.
35) Mckay, G., Blair, H. S. and Finton, A. (1986): Sorption of metal ions by chitosan, in: Immobilization of ions by biosorption. Eddles H, Hunt S, (Eds.). Ellis Herwood, Chichester, UK.
36) Mckay, G., Otterburn, M. S. and Sweeney, A. G. (1981): Surface mass transfer process during colour removal from effluent using silica. *Wat. Res.,* 15 (3): 327-331.
37) Mishra, P. C. and Patel, R. K. (2009): Removal of lead and zinc ions from water by low cost adsorbents. *J. Hazard. Mater.,* 168 (1): 319–325.
38) Mondal, M. K. (2009): Removal of Pb(II) ions from aqueous solution using activated tea waste: Adsorption on a fixed –bed column. *J. Environ. Manage.,* 90 (11): 3266- 3271.
39) Moufilh, M., Aklil, A. and Sebti, S. (2005): Removal of lead from aqueous solutions by activated phosphate. *J. Hazard. Mater.,* 119 (1-3): 183–188.
40) Nasuha, N. *et al.* (2010): Rejected tea as a potential low cost adsorbent for the removal of methylene blue. *J. Hazard. Mater.,* 175 (1-3): 126-132.
41) Odoemelam, S. A., Iroh, C. U. and Igwe, J. C. (2011): Copper (II), Cadmium (II) and Lead (II) adsorption kinetics from aqueous metal solutions using chemically modified and unmodified cocoa pod husk (Theobroma cacao) waste boimass. *Res. J. Applied Sci.,* 6 (1): 44-52.
42) Ofomaja, A. E., Unuabonah, E. I. and Oladoja, N. A. (2010): Competitive modeling for the

biosorptive removal of copper and lead ions from aqueous solution by Mansonia wood sawdust. *Bioresource Technol.,* 101 (11): 3844-3852.

43) Onundi, Y. B. *et al.* (2011): Heavy metals removal from synthetic wastewater by a novel nano-size composite adsorbent. *Int. J. Environ. Sci. Tech.,* 8 (4): 799-806.
44) Papini, M. P. *et al.* (2002): Equilibrium modeling of lead adsorption onto a ''red soil'' as a function of the liquid-phase composition. *Ind. Eng. Chem. Res.,* 41 (8): 1946–1954.
45) Rafatullah, M. *et al.* (2009): Adsorption of copper (II), chromium (III), nickel (II) and lead (II) ions from aqueous solutions by meranti sawdust. *J. Hazard. Mater.,* 170 (2-3): 969–977.
46) Renmin, G. *et al.* (2005): Effect of chemical modification on dye adsorption capacity of peanut hull. *Dyes and Pigments.,* 67 (3): 175-181.
47) Rhoades, J. D. (1982): Cation exchange capacity, in: Methods of Soil Analysis Part 2. Chemical and Microbiological Properties, second eds. American Society of Agromony/Soil Science Society of America, Madison, WI, USA.
48) Saha, P. and Sanyal, S. K. (2010): Assessment of the removal of cadmium present in wastewater using soil- admixture membrane. *Desalination,* 259 (1-3): 131-139.
49) Sari, A., Cıtak, D. and Tuzen, M. (2010): Equilibrium, thermodynamic and kinetic studies on adsorption of Sb (III) from aqueous solution using low-cost natural diatomite. *Chem. Eng. J.,* 162 (2): 521–527.
50) Slejko, F. (1985): Adsorption technology: a step by step approach to process. Eva Appl. MarcelDekker, New York.
51) Sujana, M. G., Pradhan, H. K. and Anand, S. (2009): Studies on sorption of some geomaterials for fluoride removal from aqueous solutions. *J. Hazard. Mater.,* 161 (1): 120-125.
52) Tsai, W. T. and Chen, H. R. (2010): Removal of Malachite Green from aqueous solution using low-cost chlorella-based biomass. *J. Hazard. Mater.,* 175 (1-3): 844–849.
53) Weber, W. J. and Morris, J. C. (1963): Kinetics of adsorption on carbon from solution. *J. Saint. Eng. Div. Am. Soc. Civ. Eng.,* 89: 31-60.
54) Weerasooriya, R., Aluthpatabendi, D. and Tobschall, H. J. (2001): Charge distribution multi-site complexation (CD-MUSIC) modeling of Pb (II) adsorption on gibbsite. *Colloids Surf A: Physicochem Eng. Asp.,* 189 (1): 131–144.